Clinical Immunology (2006) **120**, 189–198

available at www.sciencedirect.com

SCIENCE DIRECT®

www.elsevier.com/locate/yclim

STAT4 deficiency reduces autoantibody production and glomerulonephritis in a mouse model of lupus

Zhiwei Xu [a], Biyan Duan[a], Byron P. Croker [a,b], Laurence Morel [a,*]

[a] *Department of Pathology, Immunology, and Laboratory Medicine, University of Florida, Gainesville, FL 32601-0275, USA*
[b] *North Florida/South Georgia Veterans Health System, Gainesville, FL 32608, USA*

Received 22 November 2005; accepted with revision 24 March 2006
Available online 19 May 2006

KEYWORDS
Lupus;
Cytokines;
Mouse models;
Autoantibodies;
Glomerulonephritis;
IL-12;
IL-4

Abstract To determine the respective role of the IL-12 and IL-4 pathways in the pathogenesis of systemic lupus erythematosus, we bred the Stat4 and Stat6 null alleles onto the lupus-prone mouse B6.TC, which is a congenic derivative of NZM2410. This model is characterized by abnormal splenocyte expansion, distribution and architecture, T cell activation, peripheral B cell development, production of anti-nuclear antibodies, and proliferative glomerulonephritis. STAT4 deficiency normalized the expression of each of these disease markers toward or to C57BL/6 levels. In contrast, STAT6 deficiency impacted splenocyte expansion and architecture, T cell activation, and anti-nuclear autoantibody production, but without any significant effect on B cell development or renal pathology. These results show that the IL-12/STAT4 pathway is involved in multiple disease-associated phenotypes in the B6.TC mouse. In contrast, the IL-4/STAT6 pathway regulates only a subset of disease markers that did not affect renal pathology.

Introduction

A number of studies in patients and in murine models have reported that lupus is associated with the dysregulation of a wide variety of cytokines [1]. Within the well-characterized (NZB × NZW)F1 (BWF1) and its NZM derivative mouse models, conflicting results have been reported regarding the respective roles of IFNγ and IL-4, as the prototypic cytokines of the T helper 1 and 2 (Th1 and Th2) effector pathways. In BWF1 mice, over-expression of IFNγ, but not IL-4, significantly enhanced disease severity [2], and the immunosuppressive agent FK506 prevented lupus nephritis by suppressing IL-2 and IFNγ, but not IL-4 nor IL-10 production [3]. On the other hand, impairment of IL-4 signaling, either with anti-IL-4 Ab treatment or STAT6 deficiency dramatically ameliorated kidney disease in the NZM2410 and NZM2328 strains, in spite of the presence of high levels of anti-dsDNA antibodies [4,5]. In these NZM strains, however, STAT4 deficiency was associated with a worsening of clinical nephritis in spite of an absence of anti-dsDNA Ab. These results suggested a differential role of cytokines in lupus pathogenesis, with Th1 cytokines supporting anti-dsDNA Ab production, and Th2 cytokines promoting glomerulosclerosis.

* Corresponding author. Fax: +1 352 392 3053.
E-mail address: morel@ufl.edu (L. Morel).

1521-6616/$ – see front matter © 2006 Elsevier Inc. All rights reserved.
doi:10.1016/j.clim.2006.03.009

To dissect the genetic mechanisms by which these cytokines regulate lupus pathogenesis, we have introduced STAT4 or STAT6 deficiency on the B6.NZM.*Sle1*.*Sle2*.*Sle3* (B6.TC) lupus-prone mouse. This triple congenic strain contains the three NZM2410 lupus susceptibility loci *Sle1*, *Sle2*, and *Sle3* that are necessary and sufficient to reconstitute a fully penetrant lupus pathogenesis on a C57BL/6 (B6) background [6], and constitutes a simplified lupus genetic model since it contains only about 6% of the NZM2410 genome. The phenotypes of B6.TC.*Stat4*$^{-/-}$ and B6.TC.*Stat6*$^{-/-}$ mice were in sharp contrast with those found by others in NZM2410.*Stat4*$^{-/-}$ and NZM2410.*Stat6*$^{-/-}$, in that anti-dsDNA Ab production was reduced by both STAT4 and STAT6 deficiency, but renal pathology was significantly reduced only by STAT4 deficiency. Multiple disease markers in various cellular compartments were restored to B6 levels in B6.TC.*Stat4*$^{-/-}$, which suggests that abnormal IL-12/STAT4 signaling is responsible for these phenotypes in B6.TC mice.

Materials and methods

Mice

The production of the B6.*Sle1*.*Sle2*.*Sle3* (B6.TC) has been previously described [6]. B6.TC.*Stat4*$^{-/-}$ and B6.TC.*Stat6*$^{-/-}$ mice were produced using a marker-assisted strategy [7] to introgress the *Stat4* or *Stat6* null allele from the BALB/c.*Stat4*$^{-/-}$ or BALB/c.*Stat6*$^{-/-}$ strains (obtained from the Jackson Laboratory), respectively. BALB/c alleles were selected against using markers polymorphic between B6 and BALB/c, and mice used in this study were at $\geq$N8 backcross to the B6 background. B6 mice were obtained from the Jackson Laboratory (Bar Harbor, ME). Unless specified, both males and females between 7 and 10 months of age were used in equal number in this study. All animal protocols were approved by the Institutional Animal Care and Use Committee of the University of Florida.

Flow cytometry

Flow cytometric analysis was performed as previously described [6]. Briefly, peritoneal cavity (PerC) cells were obtained by flushing with RPMI 1640 supplemented with 10% FCS and 1 mM EDTA. Splenic single cell suspensions were prepared by removing RBCs with 0.83% NH_4Cl. Cells were blocked first with saturating amounts of anti-CD16/CD32 (2.4G2, BD Pharmingen, San Diego, CA) for 15 min in staining buffer (PBS, 5% horse serum and 0.09% sodium azide) and then stained with FITC-, PE-, or biotin-conjugated mAbs, followed by Sav-PerCP-Cy5.5 (BD Pharmingen). The following conjugated mAbs used in these experiments were purchased from BD Pharmingen: CD3e (145-2C11), CD4 (RM4-5), CD5 (53-7.3), CD8a (53-6.7), CD11b (M 1/70), CD11c (HL3), CD19 (1D3), CD23 (B3B4), CD43 (S7), CD44 (IM7), CD62L (MEL-14), CD69 (H1.2F3), CD80 (16-10A1), CD86 (GL1), CD138 (281-2), B220 (RA3-6B2), IgM^b (AF6-78), IgM^a (DS-1), IgM (II/41), I-Ab (AF6-120.1), CD93 (AA4.1), and their isotype controls. Anti-CD21 (7E9) was a gracious gift from Susan Boackle (UCHSC, Denver, Co). The stained cells were analyzed on a FACScan or FACSCalibur cytometer (BD Biosciences, Mountain View, CA). Non-viable cells were excluded on the basis of forward and side scatters characteristics. At least 20,000 events were acquired per sample.

Antibody measurements

The anti-dsDNA and anti-chromatin ELISA assays were carried out as previously described [8]. For the anti-chromatin ELISA, Immuno II plates (Thermo Labsystems, Franklin, MA) were pre-coated with methylated bovine serum albumin (Sigma, St-Louis, MO) in PBS and then coated with dsDNA (50 μg/ml) in PBS and total histone (10 μg/ml) in bi-carbonated buffer. Test sera were incubated in duplicate at 1:100 dilutions. Bound IgG was detected by alkaline phosphatase-conjugated goat anti-mouse IgG (Chemicon, Temecula, CA) and pNPP substrate (Sigma). Relative units were standardized using a positive serum from an NZM2410 mouse, arbitrarily setting the reactivity of a 1:100 dilution of this control serum to 100 units. Serum IgG1, IgG2a, IgG2b, and IgG3 isotypes were detected by sandwich ELISA. Nunc-Immuno TM plates were coated with goat IgG anti-mouse-κ and λ (9:1 ratio, Southern Biotech., Birmingham, AL) in bicarbonate buffer. After blocking with 1% BSA in Tris—HCl—NaCl, the diluted test sera (1:200,000) were incubated in duplicate. Finally, the bound IgG isotypes were detected by alkaline phosphatase-conjugated goat anti-mouse IgG1, IgG2a, IgG2b, and IgG3 (Southern Biotech.) and pNPP substrate.

Immunofluorescence of spleen sections

Spleen 8 μm cross-sections were fixed with cold acetone. Rehydrated sections were blocked with 10% rat serum and 1% BSA, and stained with CD4-PE, B220-FITC, and CD11b-APC (BD Pharmingen). Photographs were taken with a Zeiss Axioplan 2 Fluorescence microscope.

Renal pathology

Proteinuria was determined semi-quantitatively with Albustix strips (Bayer, Elkhart, IN), using a 0—4 scale (0: negative, 1: 30 mg/dl, 2: 100 mg/dl, 3: 300 mg/dl, and 4: over 2000 mg/dl of urinary protein). The type and extent of glomerular lesions were evaluated using a classification based on modifications of the WHO and RPS/ISN Classification of Glomerulonephritis in Systemic Lupus Erythematosus [9] with a semi-quantitative overlay. The glomerular classification is based on light microscopy features of mesangial matrix increase (Mm), hypercellularity limited to the mesangium (Mc), subendothelial hyaline deposits or wire loop lesions (H), proliferative or necrotizing lesions involving the capillary loops (P), subepithelial spikes (S), and normal (N). Proliferative lesions are subdivided into those involving less than 50% of the capillary bed (segmental, Ps) and those involving more than or equal to 50% of the capillary bed (global, Pg) and crescentic. The number (percentage) of glomeruli with a particular lesion is semi-quantified as +1 (1—9%), +2 (10—24%), +3 (25—49%), and +4 (greater than or equal to 50%). With this schema there is no need for a separate category of focal proliferative glomerulonephritis (less than 50% of glomeruli involved) as this would be

Table 1 Spleen weight, distribution, and activation of splenocyte subsets. B-1a cells were defined as IgM$^+$ CD5$^+$ B220^{lo}, B-2 cells as CD5$^-$ B220^{hi}, mDCs as CD11b$^+$ CD11c$^+$ and macrophages as CD11b$^+$ CD11c$^-$ splenocytes

	B6.TC	B6.TC.*Stat4*$^{-/-}$	B6.TC.*Stat6*$^{-/-}$
Spleen weight (mg)	447 ± 253	200 ± 124***	331 ± 229*
CD4$^+$ T cells (% lymphocytes)	21.03 ± 2.42	23.99 ± 2.84*	20.27 ± 3.81
CD8$^+$ T cells (% lymphocytes)	5.53 ± 2.36	10.98 ± 2.02***	8.07 ± 2.59**
CD4/CD8	4.92 ± 3.61	2.27 ± 0.47*	2.89 ± 1.38*
CD44$^+$ (% CD4$^+$)	74.81 ± 8.9	59.81 ± 7.90***	64.38 ± 12.56*
B-1a (% lymphocytes)	5.28 ± 1.29	7.46 ± 2.88*	11.37 ± 6.46*
B-2 cells (% lymphocytes)	38.12 ± 6.69	36.96 ± 8.11	38.12 ± 10.53
CD69$^+$ (% B cells)	26.04 ± 5.90	11.30 ± 3.33***	17.49 ± 6.55***
MHCII mfi (B200$^+$ gated)	781.97 ± 46.40	225.16 ± 58.32***	431.57 ± 239.05*
non-B/T cells (% splenocytes)	20.38 ± 6.73	14.43 ± 8.48*	14.89 ± 7.99*
mDC (% splenocytes)	7.47 ± 3.23	4.60 ± 2.35*	6.88 ± 3.65
Mac (% splenocytes)	12.73 ± 6.40	6.31 ± 2.07*	10.78 ± 5.5

Mean + SD of >30 mice per strain for spleen weight and 12—13 mice per strain for cell subset distribution and activation. Statistical significance is indicated in comparison to the corresponding B6.TC values.

categorized as a P3 (2 or 1) lesion. In the clinical classification, hyaline (H) is included with the proliferative category even though some predominantely hyaline lesions have minimal hypercellularity ([10] and Croker unpublished observations). This separation is particularly important in the NZ mouse strains since the hyaline lesion is the

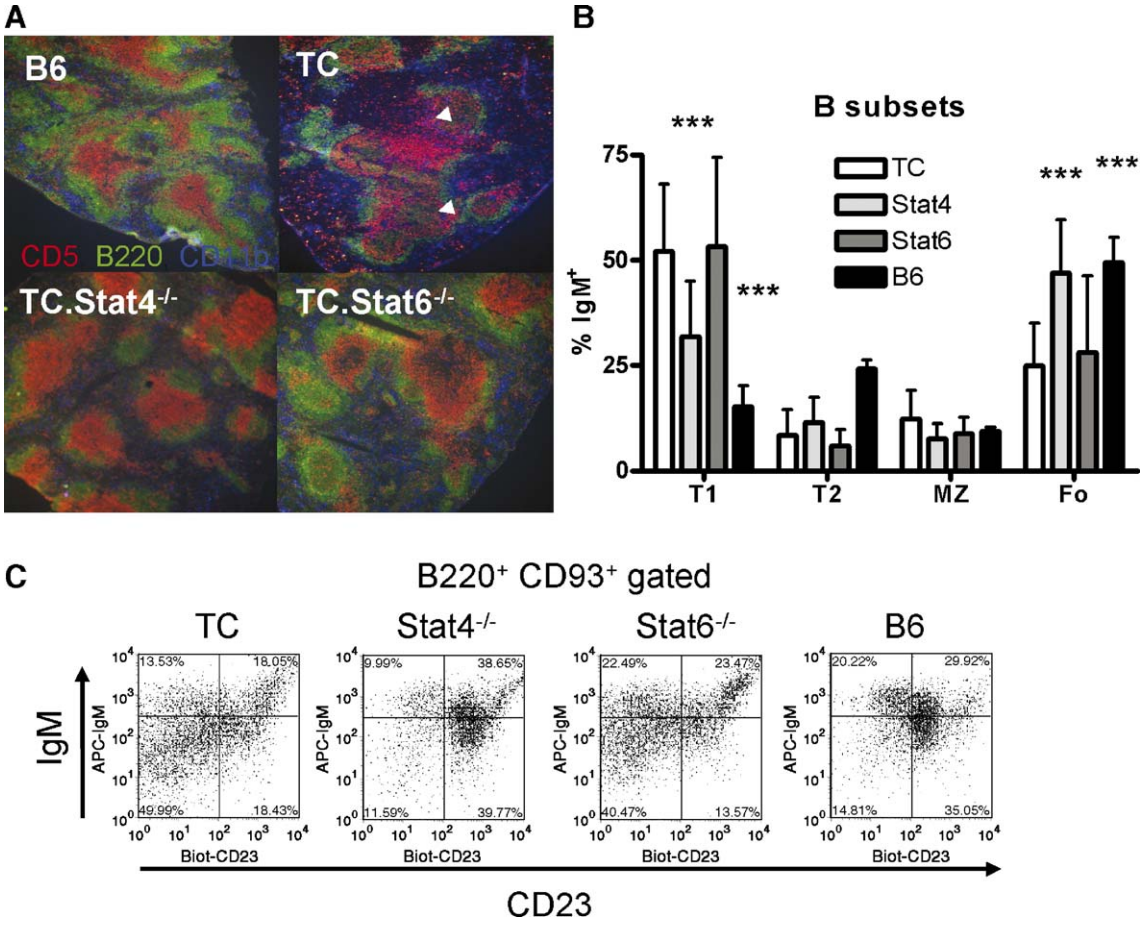

Figure 1 Effect of STAT4 and STAT6 deficiency on splenic architecture and B cell peripheral development. (A) Follicular B cells lacking in B6.TC are present in B6.TC.*Stat4*$^{-/-}$ and B6.TC.*Stat6*$^{-/-}$, and the number of CD11b$^+$ cells present in the follicles (white arrowheads) is reduced. Representative sections from at least 5 mice per strains. Magnification × 50. (B) Distribution of B cell subsets: T1 (CD21^{lo} CD23$^-$), T2 (CD21$^+$ CD23$^+$), marginal zone (MZ, CD21^{hi} CD23$^-$), and follicular (Fo, CD21^{lo} CD23$^+$) as percentages of IgM$^+$ splenocytes. Statistical significance indicates comparisons with B6.TC values. (C) Representative distribution of transitional B220$^+$ CD93$^+$ splenic B cells: T1: IgM^{hi} CD23^{lo}, T2: IgM^{hi} CD23^{hi}, and T3: IgM^{lo} CD23^{hi}.

phenotype of the NZW [11,12] and B6.NZM.*Sle2*.*Sle3* strains [6] and these mice have intermediate survival [13] between normal strains and those with proliferative lesions. In any one animal, several lesions might be present and the predominant type is used for statistical analysis.

The presence of immune complexes in the kidneys was evaluated on 8 μM frozen sections stained with FITC-conjugated anti-C3 (Cappel, Malvern, PA) and anti-IgG γ chain (Jackson Immunoresearch, West Grove, PA). Staining intensity was evaluated in a blind fashion on a semi-quantitative 0—3 scale and averaged on at least 10 glomeruli per section. For the detection of glomerular macrophages and T cells, re-hydrated 8 μM sections were first incubated with 0.6% H_2O_2 and 0.2% NaN_3 to inhibit endogerous peroxidase activity, then with blocking buffer (10% rat serum and 1% BSA), and stained with biotin-conjugated CD68 (Serotec) and CD4 (BD Pharmingen). HRP-streptavidin (Vector, Burlingame, CA) and DAB substrate were added and positive cells developed a brown color. Sections were counterstained with Mayer's hematoxylin solution (Sigma). Immunostaining was analyzed by averaging the number of CD68 or CD4 positive cells in 10 randomly selected glomeruli under high power field for each kidney section.

Cytokine detection

For immunofluorescent staining of intracellular cytokines, spleen cells from 6—8 months old mice were incubated for 5 h with PMA and ionomycin (leukocyte activation cocktail with Golgiplug, BD Pharmingen). Cells were then blocked and surface markers stained as stated above. Fixed and permeabilized cells (Cytofix/Cytoperm TM solution, BD-Pharmingen) were stained with IL-4-PE (BVD4-1D11) and IFN-γ-APC (XMG1.2), or IL-10-APC (JES5-16E3) and IL-2-PE (JES6-5H4), and analyzed on a FACSCalibur cytometer (BD Biosciences).

Statistical analysis

Data were analyzed with the GraphPad Prism 4.0 software package. Multiple comparisons between groups were conducted with Dunnett's or Dunns' multiple comparison tests using the B6.TC data as control, for parametric and non-parametric data, respectively. For specific comparisons between 2 groups, Student's *t* or Mann—Whitney tests were applied. Penetrance values were compared used χ^2 tests. Survival rates were compared with the Logrank test. Throughout the figures, significance levels are indicated as follows: $^*P < 0.05$, $^{**}P < 0.01$, and $^{***}P < 0.001$.

Results

STAT4 and STAT6 deficiency affects the distribution of lymphocyte subsets in B6.TC mice

STAT4 and STAT6 deficiency resulted in significant changes in hemapoietic cell expansion and distribution in B6.TC mice (Table 1). Spleen weights were significantly reduced in both cases, although without reaching B6 levels (mean ± SD: 87 ± 9 mg), and were lower in B6.TC.*Stat4*$^{-/-}$ than in B6.*Stat6*$^{-/-}$ mice ($P = 0.02$). B6.TC mice are characterized with an elevated CD4/CD8 ratio due to *Sle3*-mediated impaired activation induced cell death [14] and an increased level of CD4$^+$ T cell activation [6]. Both STAT4

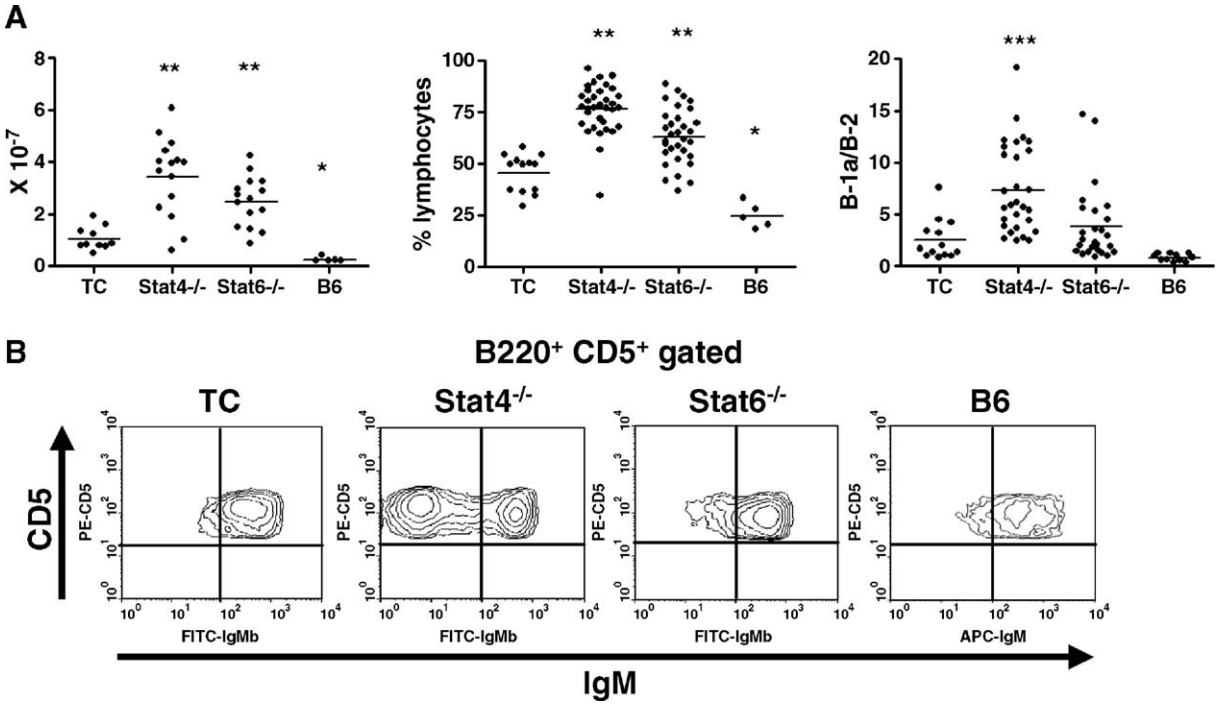

Figure 2 STAT4 and STAT6 deficiency affect perC B-1a cells. (A) B-1a absolute numbers, percentages of lymphocytes, and B-1a/B2 ratios. Statistical significance indicates comparisons with B6.TC values. (B) Representative FACS plots of B220$^+$ CD5$^+$ perC cells showing the significant increase in the IgM^{lo} population in B6.TC.*Stat4*$^{-/-}$ mice.

and STAT6 deficiency significantly decreased the CD4/CD8 ratio as compared to B6.TC, although not back to B6 levels (1.17 ± 0.4). Similarly, the percentage of effector/memory $CD44^+$ $CD4^+$ T cells was significantly decreased in both B6.TC.*Stat4*$^{-/-}$ and B6.*Stat6*$^{-/-}$ mice as compared to B6.TC (74.81 ± 8.90), and even to a level similar to B6 (51.0 ± 3.0) for STAT4 deficiency. Both STAT4 and STAT6 deficiency significantly decreased B cell activation, although to a lesser extent for STAT6.

Both STAT4 and STAT6 deficiency decreased the percentage of non-T/non-B cells, but only STAT4 deficiency impacted the percentage of splenic macrophages and myeloid DCs. Interestingly, both STAT4 and STAT6 deficiency affected the location of $CD11b^+$ myeloid cells. These cells are found in great numbers in the follicles in B6.TC mice, but restored to a B6-like distribution mostly in the red pulp in B6.TC.*Stat4*$^{-/-}$ and B6.*Stat6*$^{-/-}$ spleens (Fig. 1A).

B6.TC mice have a disorganized follicular structure, with a striking paucity in follicular B cells as compared to B6 (Fig. 1A). These histological data coincide with flow cytometry analysis showing a significantly lower level of IgM^+ $CD23^{hi}$ $CD21^{int}$ follicular (Fo) B cells and higher level of IgM^+ $CD23^{lo}$ $CD21^{int}$ transitional T1 B cells in B6.TC mice (Fig. 1B). STAT4 but not STAT6 deficiency significantly restored the T1/Fo ratio to B6 levels, which translated into well-formed B cell zones in the B6.TC.*Stat4*$^{-/-}$ splenic follicles (Fig. 1A). We examined in more detail the distribution of transitional splenic B cells using B220, CD93, IgM, and CD23 to define three T1 (IgM^{hi} $CD23^{lo}$), T2 (IgM^{hi} $CD23^{hi}$), and T3 (IgM^{hi} $CD23^{hi}$) $B220^+$ $CD93^+$ populations [15]. The majority of the cells that were initially identified as IgM^+ $CD23^{lo}$ $CD21^{int}$ T1 in B6.TC mice are in fact a yet undefined population that is $B220^+$ $CD93^+$ $CD23^{lo}$ IgM^{lo} and not IgM^{hi} (Fig. 1C). In addition, the T3 population is markedly reduced in B6.TC mice. Interestingly, STAT4 deficiency restored a B6-like distribution of transitional B cells, while STAT6 deficiency had no effect on this phenotype (Fig. 1C).

Finally, both STAT4 and STAT6 deficiency resulted in a significantly higher percentage of splenic and perC B-1a cells (Table 1 and Fig. 2). Due to the presence of the *Sle2* locus [16,17], B6.TC mice have significantly higher numbers and percentages of perC B-1a cells as compared to B6. These

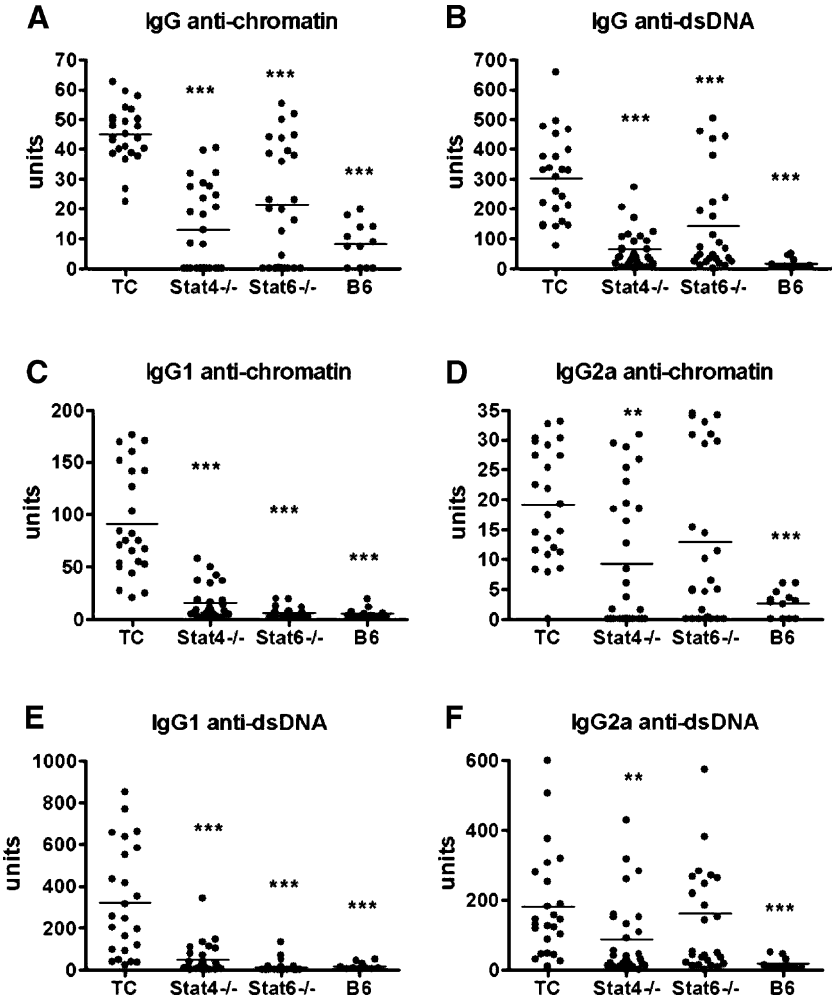

Figure 3 STAT4 and STAT6 deficiency reduce anti-nuclear IgG antibody production, but only STAT4 deficiency reduces the IgG2a isotype. Total IgG anti-chromatin (A) and anti-dsDNA (B). Anti-chromatin IgG1 (C) and IgG2a (D). Anti-dsDNA IgG1 (E) and IgG2a (F). Relative units were standardized by using a positive serum from an NZM2410 mouse, arbitrarily setting the reactivity of a 1:100 dilution of this control serum to 100 units. Statistical significance indicates comparisons with B6.TC values established with Kruskal–Wallis tests and Dunn's corrections for multiple comparisons.

values were further increased by both STAT4 and STAT6 deficiency. The B-1a/B2 ratio was, however, enhanced only in B6.TC.*Stat4*$^{-/-}$ mice, suggesting that STAT6 deficiency increased the numbers of both B-1a and B2 cells. In addition, B6.TC.*Stat4*$^{-/-}$ perC B-1a cells differ from B-1a cells in the other strains by their large proportion of IgM^{lo} cells (Fig. 2B). We have previously reported that this phenotype maps to the *Sle2a* locus, and these B-1a cells, which express high levels of CXCR5, may represent newly emigrated splenic B-1a cells [18]. The results reported here suggest that STAT4 deficiency enhances this phenotype.

Both STAT4 and STAT6 deficiency decreased autoantibody production

As their parental strain NZM2410, B6.TC mice secrete high levels of immunoglobulin and anti-nuclear autoantibodies [6]. STAT4 and STAT6 deficiency significantly decreased IgG levels and STAT4 deficiency affected all isotypes ($P < 0.01$), while STAT6 deficiency decreased only IgG1 ($P < 0.001$) and IgG2b ($P < 0.01$). Anti-chromatin and anti-dsDNA IgG levels were significantly reduced in both B6.TC.*Stat4*$^{-/-}$ and B6.TC.*Stat6*$^{-/-}$ mice, either considering titers (Figs. 3A and B), or penetrance (45% and 54% anti-dsDNA positive in B6.TC.*Stat4*$^{-/-}$ and B6.TC.*Stat6*$^{-/-}$ mice, respectively, compared to 100% B6.TC positive, $P < 0.01$). The anti-dsDNA IgG level was significantly lower in B6.TC.*Stat4*$^{-/-}$ than in B6.TC.*Stat6*$^{-/-}$ mice ($P < 0.013$), but not as low as that in age-matched B6 controls ($P < 0.012$). Interestingly, anti-chromatin and anti-dsDNA IgG1 antibodies were significantly reduced in both B6.TC.*Stat4*$^{-/-}$ and B6.TC.*Stat6*$^{-/-}$ mice (Figs. 3C and E), while the IgG2a isotype for these specificities was only significantly decreased in B6.TC.*Stat4*$^{-/-}$ mice (Figs. 3D and F). The decrease of IgG2a

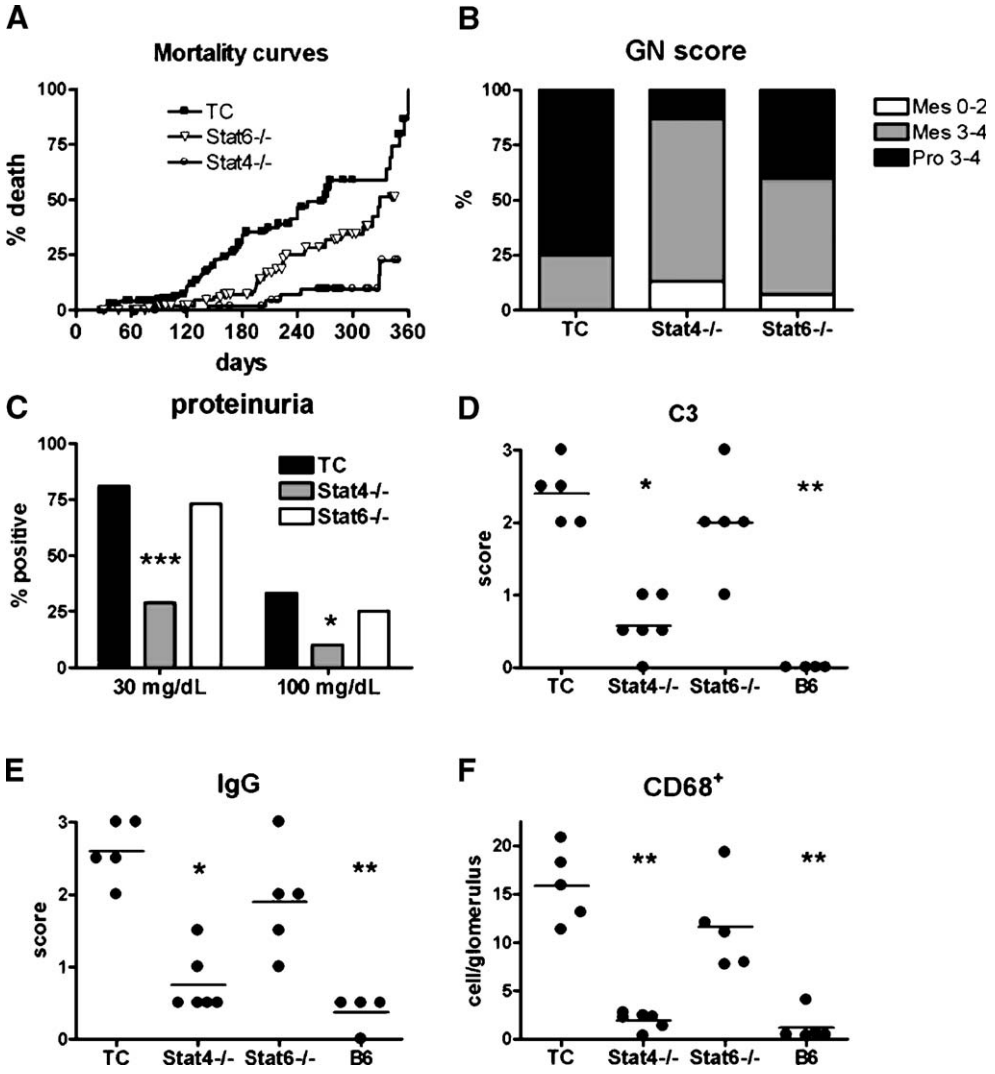

Figure 4 Survival and renal pathology of B6.TC.*Stat4*$^{-/-}$ and B6.TC.*Stat6*$^{-/-}$ mice comparatively to B6.TC and B6. (A) Mortality curves for 201 B6.TC, 53 B6.TC.*Stat4*$^{-/-}$, and 53 B6.TC.*Stat6*$^{-/-}$ mice followed up to 12 months of age. (B) Distribution of the GN score graded as either mesangial (Mes) or proliferative (Pro) and grouped by severity 0—2 and 3—4 (see Materials and methods). Fifteen mice were scored for each strain at 9 months of age. (C) Percentage of mice showing a proteinuria of at least 30 mg/dl or 100 mg/dl by 9 months of age (30 mice per strain). Semi-quantitative scoring of complement C3 (D) and IgG (E) deposition in the glomeruli. (F) Average number of CD68+ macrophage per glomerulus. Statistical significance indicated in panels C—F corresponds to comparisons with B6.TC mice.

anti-nuclear antibodies is, however, small and does not reach down to B6 levels.

STAT4 deficiency increased survival and decreased renal pathology

STAT4 deficiency was associated with a significant improvement in survival as compared to B6.TC mice ($P < 0.0001$) (Fig. 4A). STAT6 deficiency also increased survival ($P < 0.0001$), but survival was significantly longer in B6.TC.*Stat4*$^{-/-}$ than in B6.TC.*Stat6*$^{-/-}$ mice ($P < 0.004$). STAT4 deficiency also decreased the severity of glomerular lesions as illustrated in Fig. 5 and quantified in Fig. 4B. GN scores were significantly lower in B6.TC.*Stat4*$^{-/-}$ ($P = 0.006$) and reflected a shift to a less cellular phenotype with mesangial matrix expansion (Mm). Clinically, the percentage of B6.TC.*Stat4*$^{-/-}$ mice showing proteinuria (either greater than 30 mg/dl or greater than 100 mg/dl) was significantly lower than in age-matched B6.TC mice (Fig. 4C). These findings were corroborated by a significant reduction in C3 (Fig. 4D, $P < 0.05$) and IgG (Fig. 4E, $P < 0.05$) glomerular deposits, as illustrated in Fig. 5. We have recently associated the presence of intra-glomerular macrophages with severe renal pathology in B6.TC mice [18]. Macrophages were largely absent from B6.TC.*Stat4*$^{-/-}$ glomeruli (Fig. 4F, $P < 0.01$), which were comparable to B6 kidneys (Fig. 5). $CD4^+$ T cells were also found in B6.TC glomeruli, and these values were significantly ($P < 0.01$) reduced to B6 levels by STAT4 deficiency (Fig. 4). Comparatively, STAT6 deficiency had a relatively small impact on B6.TC renal pathology as

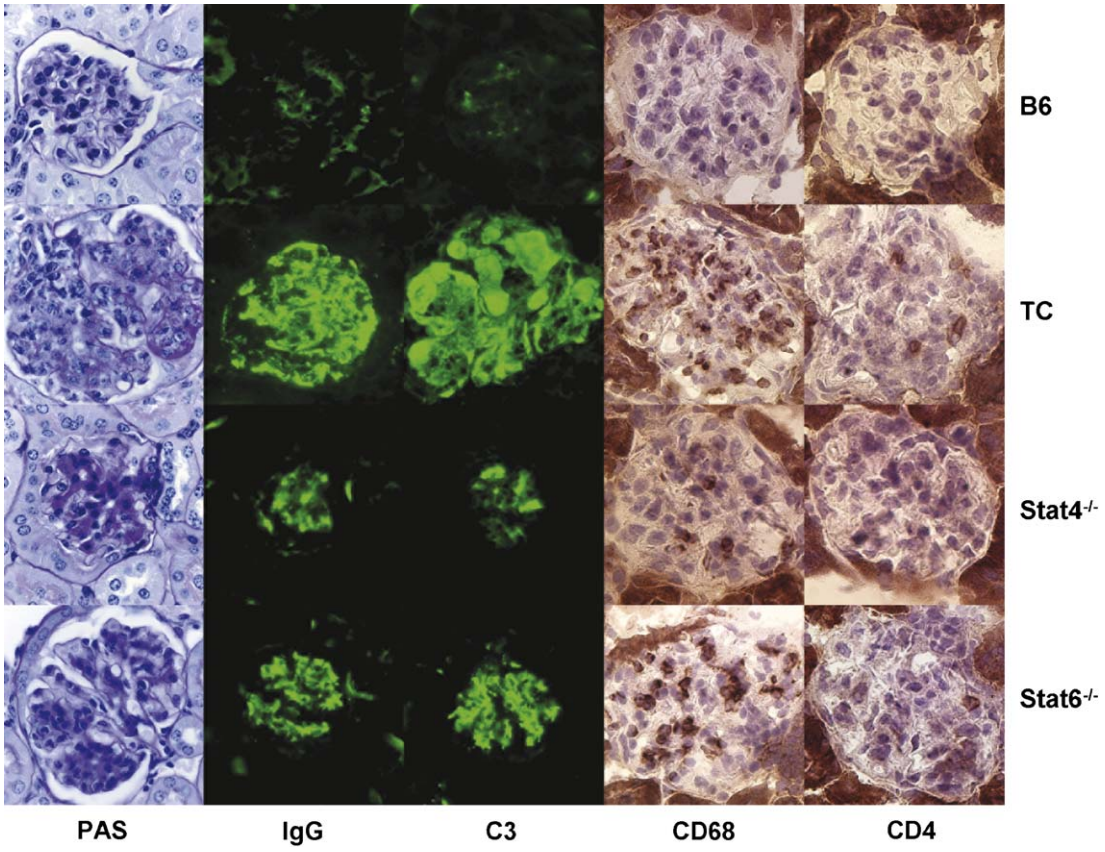

Figure 5 Representative renal pathology in B6.TC.*Stat4*$^{-/-}$ and B6.TC.*Stat6*$^{-/-}$ mice comparatively to B6.TC and B6. From left to right, representative glomeruli stained with PAS, anti-C3, -IgG, -CD68, and -CD4 antibodies. All images are taken with 100× oil immersion lens and are size-matched for the PAS stains: (B6) This image shows a normal (N) glomerulus. The vascular pole is at 8 o'clock and the tubular pole is at 3. Note the size of the glomerulus, cellularity and mesangium. IgG, C3, CD68, and CD4 show background staining. (B6.TC) This glomerulus was classified as proliferative-global (Pg). The vascular pole is 10—11 o'clock. The glomerulus is enlarged with hypercellularity. Note that many of the nuclei are enlarged. There is a wire loop lesion (subendothelial deposit) at 4 o'clock. This is representative of marked inflammation and cellularity in the TC glomerulonephritis. This is accompanied by large mesangial and capillary IgG and C3 deposits. Numerous dark CD68 positive cells are present with a few CD4 staining cells. (B6.TC.*Stat4*$^{-/-}$) This glomerulus was classified as mesangiopathic-matrix (Mm). The vascular pole and macula densa are at 3 o'clock. The glomerular dimensions and cellularity are similar to normal but there is an increase in matrix. This image is representative of the B6.TC.*Stat4*$^{-/-}$ glomerulonephritis with increased mesangium with IgG and C3 deposits but little or no cellularity or inflammation. CD68 shows few staining cells and CD4 shows background staining. (B6.TC.*Stat6*$^{-/-}$) This glomerulus was classified as proliferative-segmental (Ps). The vascular pole is at 4 o'clock. There is a segmental hypercellularity with obliteration of the capillary lumens in the left lower third of the glomerular capillary bed and some overall enlargement. This image is representative of the B6.TC.*Stat6*$^{-/-}$ strain with increased cellularity and matrix with IgG and C3 deposits. Numerous CD68 and few CD4 staining cells are present.

measured by the criteria listed above (Figs. 4 and 5). The number of intra-glomerular macrophages and T cells was not decreased in B6.TC.*Stat6*$^{-/-}$ as compared to B6.TC. Furthermore, the frequency of glomerular hypercellularity was significantly decreased by STAT4 ($P < 0.02$) but not by STAT6 deficiency.

STAT4 and STAT6 deficiency affected cytokine secretion by B6.TC T cells

Cytokine production by TC CD4$^+$ T cells in response to PMA and ionomycin differed significantly from that of B6 CD4$^+$ T cells (Fig. 6). In response to PMA and ionomycin, TC INFγ, IL-4, and IL-10 secretion was significantly increased, while IL-2 was significantly decreased as compared to B6 T cells. Interestingly, in all cases, STAT4 deficiency restored B6.TC CD4$^+$ T cell cytokine production to B6 levels. It is noteworthy that STAT4 deficiency was not associated with a decreased IFNγ production, which was actually higher in anti-CD3 and anti-CD28 stimulated T cells. STAT6 deficiency resulted in a reduced production of INFγ and IL-10, but had no effect on IL-4 and IL-2.

Discussion

We have shown in this study that STAT4 deficiency greatly reduced clinical disease severity, and dramatically affected the expression of most disease markers in the lupus prone B6.TC mouse. Through the detailed analyses of NZM2410 congenics, we have shown that the *Sle1*, *Sle2*, and *Sle3* loci mediate lupus susceptibility through intrinsic defects in B and T lymphocytes and myeloid cells [17,19,20]. Our results here show that STAT4 deficiency normalizes the phenotypes of all these 3 cellular compartments. STAT4 is the principal signaling effector of the IL-12 receptor and its deficiency results in a severe impairment of IL-12 responses and Th1 induction [21]. IL-12R subunits and STAT4 are expressed on T cells, NK cells, and myeloid cells [22], but also on splenic B cells [23,24], although at a lower level. STAT4 deficiency in the lupus prone B6.TC mouse significantly reduced the number of intra-follicular myeloid cells, T cell activation, and elevated CD4/CD8 ratio, this latter phenotype being mediated by *Sle3*-expressing DCs [20]. We found that B cell development was also profoundly affected in B6.TC mice, with a significant skewing toward transitional CD93$^+$ stages at the expense of mature follicular subset in the spleen, and toward the B-1a compartment in the peritoneal cavity. STAT4 deficiency remarkably restored a B6-like development of the transitional to follicular stages in the spleen, which was associated in the restitution of a normal follicular architecture. In addition, the production of anti-dsDNA and anti-chromatin Ig Ab was largely abrogated and renal pathology was greatly diminished by STAT4 deficiency. A relatively modest, but significant decreased in anti-dsDNA IgG2a Ab in B6.TC.*Stat4*$^{-/-}$ could be one of the contributing factors to the decreased renal pathology. A decrease in IgG2a production has been found to significantly ameliorate renal disease independently from IFNγ production, suggesting that IgG2a is associated with increased pathogenicity [25].

The association between normalization of T cell activation, CD4/CD8 ratio, B cell peripheral development and myeloid cells follicular localization and significant reduction in autoantibody production and renal pathology validates the participation of the phenotypes in lupus pathogenesis of our model. In contrast, the increased number and propor-

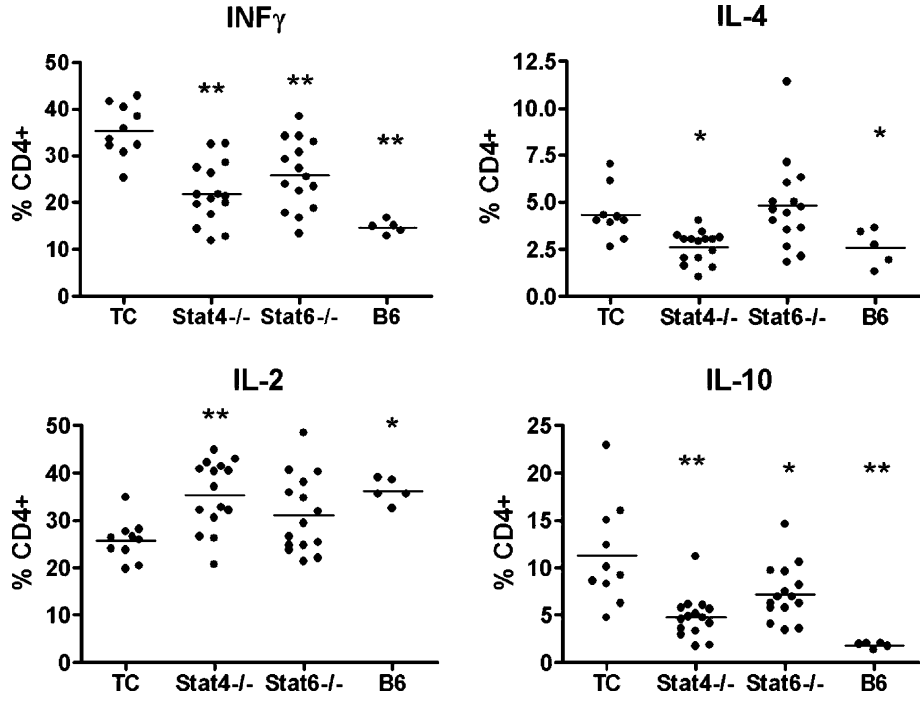

Figure 6 STAT4 and STAT6 effects on CD4$^+$ T cells cytokine production. Intra-cellular IFNγ, IL-4, IL-2, and IL-10 levels in CD4$^+$ splenocytes stimulated with PMA and ionomycin. Statistical significance indicates comparisons with TC values established with Dunnett's multiple comparison tests.

tion of B-1a cells in B6.TC.*Stat4*$^{-/-}$ mice argues against this compartment playing a critical role in the disease process. The role of IL-12 in B-1 cell development and activation is controversial. IL-12 binds to murine peritoneal B-1 cells [26]. In vivo IL-12 treatment resulted in loss of total peritoneal cavity B cells [27]. An in vitro study, however, showed that IL-12 was a survival factor for both B2 and B1 cells, but was specifically required by B-1a, but not B-2 cells for Ab production [28]. In addition, IL-12 is required for B-1 cells to produce IL-10, and it has been suggested that IL-12 increased levels with age are directly responsible for the age-related accumulation of peritoneal B1a cells [29]. The intriguing ability of B-1 cells to prevent dendritic cells to produce IL-12 has been recently revealed [30], which should prompt further research on the interactions between these two cell types.

Overall, these results are consistent with the IL-12 pathway playing a major role in the pathogenesis of the B6.TC mouse. Several cellular compartments were affected, and further studies will be necessary to determine the mechanisms by which abrogation of IL-12 signaling through STAT4 induced such changes, either directly or indirectly. As for many cytokines, the role of IL-12 in lupus is complex and controversial, with reports of both protective or enhancing effects [31]. A defect in macrophage production of IL-12 has been found in both MRL and NZB/W [32]. In NZB/W, this impaired production has been recently linked to elevated cytoplasmic IκB, resulting in a blocking of *IL-12p40* transcription by c-Rel [33]. These mice are, however, able to produce IL-12, with a strong induction in response to bacterial DNA or CpG treatment [34]. Primary genetic defects in proximal members of the IL-12/STAT4 pathway are, however, not responsible for the observed phenotype. *IL12p40* has been recently proposed as a candidate gene for *Idd4* in the NOD mouse [35], and that region of chromosome (chr.) 11 has been linked to SLE in the NZM2410 strain [36]. In the B6.TC mouse, however, *Il12p40*, *Stat4* (proximal chr. 1), *Il12rb1* (chr. 8), and *Il12rb2* (chr. 6) are all from B6 origin. Interestingly, B6.TC.*Stat4*$^{-/-}$ T cells produced abundant amounts of IFNγ, which also eliminates this cytokine as a direct candidate to account for the beneficial effects of STAT4 deficiency. Reduced but substantial amounts of IFNγ were also found in the absence of STAT4 in the RIP-LCMV model of diabetes [37]. It suggests that STAT4-independent or IL-12-independent pathways of IFNγ induction are enhanced in the B6.TC models, and this could by itself contribute to an abnormal regulation of inflammatory cytokines. In addition, B6.TC CD4^{+} T cells were deficient in IL-2 production and STAT4 deficiency restored normal IL-2 production. Low IL-2 levels can significantly contribute to lupus pathogenesis through impaired activation-induced cell death and impaired generation or maintenance of regulatory subsets. Impaired IL-2 production by human T cells from lupus patients has recently been attributed to anti-TCR/CD3 IgG antibodies that increase CREM binding [38]. Further investigation in our model should establish whether the same mechanism is involved.

STAT6 deficiency also resulted in significant changes in B6.TC mice. Their spleen weight and amount of non-B/T cells were reduced by about 25%, and their follicular architecture was normalized. The CD4/CD8 ratio, T cell activation, and anti-nuclear Ab production were significantly reduced, suggesting that IL-4 plays a role in these phenotypes. B cell development was, however, largely unchanged from B6.TC, except an increased B-1a cell population. Finally, renal disease markers were only slightly decreased by STAT6 deficiency without reaching statistical significance. These results are in sharp contrast with the results obtained with NZM2410 and NZM2328 [4,5], in which IL-4 was shown to play a major role in promoting kidney disease. Different genetic backgrounds are the most likely explanation for this discrepancy, as the *Sle* loci are on a B6 background in the B6.TC mouse, instead of a mixture of NZB and NZW genomes. Different genetic backgrounds can affect profoundly the clinical outcome of the *Sle* loci (Croker et al., in preparation). In addition, the amount and location of BALB/c genomic contamination (linked to the *Stat4*$^{-/-}$ and *Stat6*$^{-/-}$ alleles), which is likely to be different in the two studies, may also contribute to this discrepancy.

Overall, our results show that the IL-12/STAT4 pathway is involved in many of the lupus-associated phenotypes in the B6.TC mice. The dissection of the functional and genetic mechanisms by which it is achieved should reveal new regulatory pathways that are dysregulated by the expression of the *Sle* loci. Moreover, our results show that STAT4 is a promising target to modulate systemic autoimmunity, at least in specific genetic backgrounds. Statins have been shown recently to inhibit STAT4 and to be effective in treating EAE [39] and collagen-induced arthritis [40], and our results suggest that SLE may also benefit from statin treatment. Statin therapy may be associated, however, with anti-nuclear antibody production and lupus-like syndrome [41]. Elucidation of the genetic interactions supporting the beneficial effect of inhibiting either the STAT4 or STAT6 pathways will be crucial in the validation of these potential targets and prevents adverse reactions.

Acknowledgment

This work was supported by an NIH grant RO1-AI058150 (L.M.).

References

[1] J.S. Smolen, G. Steiner, M. Aringer, Anti-cytokine therapy in systemic lupus erythematosus, Lupus 14 (2005) 189–191.
[2] K. Hasegawa, T. Hayashi, K. Maeda, Promotion of lupus in NZB × NZWF1 mice by plasmids encoding interferon (IFN-γ) but not by those encoding interleukin (IL)-4, J. Comp. Pathol. 127 (2002) 1–6.
[3] M. Sugiyama, M. Funauchi, T. Yamagata, Y. Nozaki, B.S. Yoo, S. Ikoma, K. Kinoshita, A. Kanamaru, Predominant inhibition of Th1 cytokines in New Zealand black/white F1 mice treated with FK506, Scand. J. Immunol. 33 (2004) 108–114.
[4] C.O. Jacob, S. Zang, L. Li, V. Ciobanu, F. Quismorio, A. Mizutani, M. Satoh, M. Koss, Pivotal role of Stat4 and Stat6 in the pathogenesis of the lupus-like disease in the New Zealand mixed 2328 mice, J. Immunol. 171 (2003) 1564–1571.
[5] R.R. Singh, V. Saxena, S. Zang, L. Li, F.D. Finkelman, D.P. Witte, C.O. Jacob, Differential contribution of IL-4 and STAT6 vs. STAT4 to the development of lupus nephritis, J. Immunol. 170 (2003) 4818–4825.
[6] L. Morel, B.P. Croker, K.R. Blenman, C. Mohan, G. Huang, G. Gilkeson, E.K. Wakeland, Genetic reconstitution of systemic

lupus erythematosus immunopathology with polycongenic murine strains, Proc. Natl. Acad. Sci. U. S. A. 97 (2000) 6670–6675.
[7] E. Wakeland, L. Morel, K. Achey, M. Yui, J. Longmate, Speed congenics: a classic technique in the fast lane (relatively speaking), Immunol. Today 18 (1997) 472–477.
[8] C. Mohan, E. Alas, L. Morel, P. Yang, E.K. Wakeland, Genetic dissection of SLE pathogenesis-Sle1 on murine chromosome 1 leads to a selective loss of tolerance to H2A/H2B/DNA subnucleosomes, J. Clin. Invest. 101 (1998) 1362–1372.
[9] J.J. Weening, V.D. D'Agati, M.M. Schwartz, S.V. Seshan, C.E. Alpers, G.B. Appel, J.E. Balow, J.A. Bruijn, T. Cook, F. Ferrario, A.B. Fogo, E.M. Ginzler, L. Hebert, G. Hill, P. Hill, J.C. Jennette, N.C. Kong, P. Lesavre, M. Lockshin, L.M. Looi, H. Makino, L.A. Moura, M. Nagata, The classification of glomerulonephritis in systemic lupus erythematosus revisited, J. Amer. Soc. Nephrol. 15 (2004) 241–250.
[10] V.D. D'Agati, Renal disease in systemic lupus erythematosus, mixed connective tissue disease, Sjögren's Syndrome, and Rheumatoid Arthritis, 5th ed., 1998, pp. 541–624.
[11] I.M. Braverman, Study of autoimmune disease in New Zealand mice: I. Genetic features and natural history of NZB, NZY and NZW strains and NZB-NZW hybrids, J. Invest. Dermatol. 50 (1968) 483–499.
[12] V.E. Kelley, A. Winkelstein, Age- and sex-related glomerulonephritis in New Zealand white Mice, Clin. Imm. Immunopath. 16 (1980) 142–150.
[13] G. Fernandes, E.J. Yunis, R.A. Good, Age and genetic influence on immunity in NZB and autoimmune-resistant mice, Clin. Immunol. Immunopathol. 6 (1976) 318–333.
[14] C. Mohan, Y. Yu, L. Morel, P. Yang, E.K. Wakeland, Genetic dissection of Sle pathogenesis: Sle3 on murine chromosome 7 impacts T cell activation, differentiation, and cell death, J. Immunol. 162 (1999) 6492–6502.
[15] D. Allman, R.C. Lindsley, W. DeMuth, K. Rudd, S.A. Shinton, R.R. Hardy, Resolution of three nonproliferative immature splenic B cell subsets reveals multiple selection points during peripheral B cell maturation, J. Immunol. 167 (2001) 6834–6840.
[16] C. Mohan, L. Morel, P. Yang, E.K. Wakeland, Genetic dissection of systemic lupus erythematosus pathogenesis-Sle2 on murine chromosome 4 leads to B cell hyperactivity, J. Immunol. 159 (1997) 454–465.
[17] Z. Xu, E.J. Butfiloski, E.S. Sobel, L. Morel, Mechanisms of peritoneal B-1a cells accumulation induced by murine lupus susceptibility locus Sle2, J. Immunol. 173 (2004) 6050–6058.
[18] Z. Xu, B. Duan, B.P. Croker, E.K. Wakeland, L. Morel, Genetic dissection of the murine lupus susceptibility locus Sle2: contributions to increased peritoneal B-1a cells and lupus nephritis map to different loci, J. Immunol. 175 (2005) 936–943.
[19] E.S. Sobel, M. Satoh, W.F. Chen, E.K. Wakeland, L. Morel, The major murine systemic lupus erythematosus susceptibility locus Sle1 results in abnormal functions of both B and T cells, J. Immunol. 169 (2002) 2694–2700.
[20] J.K. Zhu, X.B. Liu, C. Xie, M. Yan, Y. Yu, E.S. Sobel, E.K. Wakeland, C. Mohan, T cell hyperactivity in lupus as a consequence of hyperstimulatory antigen-presenting cells, J. Clin. Invest. (2005), doi:10.1172/JCI23049.
[21] M.H. Kaplan, Y.L. Sun, T. Hoey, M.J. Grusby, Impaired IL-12 responses and enhanced development of Th2 cells in Stat4-deficient mice, Nature 382 (1996) 174–177.
[22] W.T. Watford, B.D. Hissong, J.H. Bream, Y. Kanno, L. Muul, J.J. O'Shea, Signaling by IL-12 and IL-23 and the immunoregulatory roles of STAT4, Immunol. Rev. 202 (2005) 139–156.
[23] T. Yoshimoto, K. Takeda, T. Tanaka, K. Ohkusu, S. Kashiwamura, H. Okamura, S. Akira, K. Nakanishi, IL-12 up-regulates IL-18 receptor expression on T cells, Th1 cells, and B cells: synergism with IL-18 for IFN-gamma production, J. Immunol. 161 (1998) 3400–3407.
[24] E. Kuroda, T. Kito, U. Yamashita, Reduced expression of STAT4 and IFN-gamma in macrophages from BALB/c mice, J. Immunol. 168 (2002) 5477–5482.
[25] S.L. Peng, S.J. Szabo, L.H. Glimcher, T-bet regulates IgG class switching and pathogenic autoantibody production, Proc. Natl. Acad. Sci. U. S. A. 99 (2002) 5545–5550.
[26] L.A. Vogel, L.C. Showe, T.L. Lester, R.M. Mcnutt, V.H. VanCleave, D.W. Metzger, Direct binding of IL-12 to human and murine B lymphocytes, Int. Immunol. 8 (1996) 1955–1962.
[27] L.A. Vogel, T.L. Lester, V.H. VanCleave, D.W. Metzger, Inhibition of murine B1 lymphocytes by interleukin-12, Eur. J. Immunol. 26 (1996) 219–223.
[28] B.M. Jones, Effect of 12 neutralizing anti-cytokine antibodies on in vitro activation of B-cells. Interleukin-12 is required by B1a but not B2 cells, Scand. J. Immunol. 43 (1996) 64–72.
[29] N.F.L. Spencer, R.A. Daynes, IL-12 directly stimulates expression of IL-10 by CD5(+) B cells and IL-6 by both CD5(+) and CD5(−) B cells: possible involvement in age-associated cytokine dysregulation, Int. Immunol. 9 (1997) 745–754.
[30] C.M. Sun, E. Deriaud, C. Leclerc, R. Lo-Man, Upon TLR9 signaling, CD5+ B cells control the IL-12-dependent Th1-priming capacity of neonatal DCs, Immunity 22 (2005) 467–477.
[31] R. Segal, M. Dayan, H. Zinger, B. Habut, G.M. Shearer, E. Mozes, The effect of IL-12 on clinical and laboratory aspects of experimental SLE in young and aging mice, Exp. Gerontol. 38 (2003) 661–668.
[32] D.G. Alleva, S.B. Kaser, D.I. Beller, Intrinsic defects in macrophage IL-12 production associated with immune dysfunction in the MRL/++ and New Zealand Black/White F-1 lupus-prone mice and the Leishmania major-susceptible BALB/c strain, J. Immunol. 161 (1998) 6878–6884.
[33] J.J. Liu, D.I. Beller, Distinct pathways for NF-kappa B-regulation are associated with aberrant macrophage IL-12 production in lupus- and diabetes-prone mouse strains, J. Immunol. 170 (2003) 4489–4496.
[34] G.S. Gilkeson, J. Conover, M. Halpern, D.S. Pisetsky, A. Feagin, D.M. Klinman, Effects of bacterial DNA on cytokine production by (NZB/NZW)F-1 mice, J. Immunol. 161 (1998) 3890–3895.
[35] P.B. Simpson, M.S. Mistry, R.A. Maki, W.D. Yang, D.A. Schwarz, E.B. Johnson, F.M. Lio, D.G. Alleva, Cutting edge: diabetes-associated quantitative trait locus, Idd4, is responsible for the IL-12p40 overexpression defect in nonobese diabetic (NOD) mice, J. Immunol. 171 (2003) 3333–3337.
[36] L. Morel, C. Mohan, Y. Yu, J. Schiffenbauer, U.H. Rudofsky, N. Tian, J.A. Longmate, E.K. Wakeland, Multiplex inheritance of component phenotypes in a murine model of lupus, Mamm. Genome 10 (1999) 176–181.
[37] A. Holz, A. Bot, B. Coon, T. Wolfe, M.J. Grusby, M.G. von Herrath, Disruption of the STAT4 signaling pathway protects from autoimmune diabetes while retaining antiviral immune competence, J. Immunol. 163 (1999) 5374–5382.
[38] Y.T. Juang, Y. Wang, E.E. Solomou, Y. Li, C. Mawrin, K. Tenbrock, V.C. Kyttaris, G.C. Tsokos, Systemic lupus erythematosus serum IgG increases CREM binding to the IL-2 promoter and suppresses IL-2 production through CaMKIV, J. Clin. Invest. 115 (2005) 996–1005.
[39] S. Youssef, O. Stuve, J.C. Patarroyo, P.J. Ruiz, J.L. Radosevich, E.M. Hur, M. Bravo, D.J. Mitchell, R.A. Sobel, L. Steinman, S.S. Zamvil, The HMG-CoA reductase inhibitor, atorvastatin, promotes a Th2 bias and reverses paralysis in central nervous system autoimmune disease, Nature 420 (2002) 78–84.
[40] B.P. Leung, N. Sattar, A. Crilly, M. Prach, D.W. McCarey, H. Payne, R. Madhok, C. Campbell, J.A. Gracie, F.Y. Liew, I.B. McInnes, A novel anti-inflammatory role for simvastatin in inflammatory arthritis, J. Immunol. 170 (2003) 1524–1530.
[41] B. Noël, R.G. Panizzon, Lupus-like syndrome associated with statin therapy, Dermatology 208 (2004) 276–277.